



HAL
open science

Nonlinear Harmonic Analysis of a Blade Model Subjected to Large Geometrical Deflection and Internal Resonance

Nicolas Di Palma, Adrien Martin, Fabrice Thouverez, Vivien Courtier

► **To cite this version:**

Nicolas Di Palma, Adrien Martin, Fabrice Thouverez, Vivien Courtier. Nonlinear Harmonic Analysis of a Blade Model Subjected to Large Geometrical Deflection and Internal Resonance. Proceedings of ASME Turbo Expo 2019: Turbomachinery Technical Conference and Exposition, Jun 2019, Phoenix, United States. 10.1115/GT2019-91213 . hal-02159855

HAL Id: hal-02159855

<https://hal.science/hal-02159855>

Submitted on 6 Jan 2020

HAL is a multi-disciplinary open access archive for the deposit and dissemination of scientific research documents, whether they are published or not. The documents may come from teaching and research institutions in France or abroad, or from public or private research centers.

L'archive ouverte pluridisciplinaire **HAL**, est destinée au dépôt et à la diffusion de documents scientifiques de niveau recherche, publiés ou non, émanant des établissements d'enseignement et de recherche français ou étrangers, des laboratoires publics ou privés.

Nonlinear Harmonic Analysis of a Blade Model Subjected to Large Geometrical Deflection And Internal Resonance

Nicolas Di Palma^(a,b), Adrien Martin^(a), Fabrice Thouverez^(a), Vivien Courtier^(b)

^(a) École Centrale de Lyon, Laboratoire de Tribologie et Dynamique des Systèmes, Écully, France

^(b) Safran Aircraft Engines, Moissy-Cramayel, France

Email: nicolas.di-palma@ec-lyon.fr

ABSTRACT

This paper is devoted to the study of the nonlinear harmonic response of an industrial blade model subjected to large geometrical deflection. A reduction procedure is performed on the blade model using the linear normal modes of the structure. Geometrical nonlinear effects are taken into account by considering cubic and quadratic stiffnesses in the dynamical reduced model. Reduced nonlinear stiffness coefficients are computed with the STiffness Evaluation Procedure (STEP) and periodic solutions are sought using the Harmonic Balance Method (HBM) coupled to a pseudo-arclength continuation. Along with the harmonic response, a bifurcation analysis is performed to compute both turning and branching points. Specific attention is paid to the internal resonance phenomenon. 2 to 1 internal resonance occurred during the frequency response analysis close to the first and second modes of the reduced model. Mode coupling phenomena occurred during the harmonic analysis and secondary branches of solutions were obtained from branching point bifurcations.

NOMENCLATURE

$\mathbf{x}(t)$	Vector of unknowns in the physical basis
$\mathbf{M}, \mathbf{C}, \mathbf{K}$	Mass, damping and linear stiffness matrices
$\mathbf{f}^{\text{nl}}, \mathbf{f}^{\text{ext}}$	External and nonlinear forces
\mathbf{q}	Vector of unknowns in the modal basis
Φ	Truncated modal basis
$\tilde{\bullet}$	Variables in the modal basis
$\mathbf{K}^c, \mathbf{K}^q$	Quadratic and cubic reduced stiffness tensors
$\hat{\bullet}$	Vector of Fourier coefficients
N_h	Number of harmonics
\mathbf{Z}	Dynamic stiffness matrix
$\mathbf{F}, \bar{\mathbf{F}}$	Direct and inverse discrete Fourier transform matrices
s	Arc-length parameter
HBM	Harmonic Balance Method
STEP	STiffness Evaluation Procedure
DOF	Degree Of Freedom
AFT	Alternating Frequency-Time
BP, TP	Branching and Turning Points

INTRODUCTION

The aeronautic industry is constantly confronted by economic and environmental issues, such as gas emission and noise level reduction, and the need to decrease fuel consumption. The development of high-bypass ratio machines is a current trend in engine design intended to reach such objectives. This has led to the conception of slender components including fan blades which may undergo large deflections. In such conditions,

the response of the blades to harmonic excitation can involve mode couplings leading to so-called internal resonances.

Internal resonances are a feature of nonlinear systems. Having no counterpart in linear systems, they correspond to an exchange of energy between several modes of a structure. They occur when two or more frequencies of the structure are commensurable or nearly commensurable [1], which can be summarized by the following condition,

$$\sum_k m_k \omega_k \approx 0 \quad m_k \in \mathbb{Z}, k \geq 2 \quad (1)$$

where the frequencies ω_k need not be the linear frequencies of the structure [2].

Understanding internal resonance phenomena is essential in the design process of the components mentioned previously. As such phenomena are usually encountered during experimental trials, being able to predict and simulate them may lead to considerable savings of money and time. Several approaches to study internal resonance phenomenon can be found in the literature. The multiple scales analysis [1] is commonly used and furnishes pertinent results for small nonlinear systems [1, 3, 4]. However, its application is limited to weak nonlinear systems. Furthermore, multiple scales analysis is an analytical approach, then, its use for large systems is not feasible. Boivin et al. proposed in [5] an approach based on multi-mode invariant manifolds to treat interactions between modes [6, 7]. In [2, 8], internal resonances were obtained for nonlinear normal modes (NNM) calculation by a shooting method. In addition, King and Vakakis proposed in [9] an energy-based approach to compute resonant NNM. Moreover, frequency-based methods like the Harmonic Balance Method (HBM), have shown promising results concerning internal resonances [10, 11]. Though these methods have been able to predict modal interactions through internal resonance with good precision, there is little in the literature on their application to industrial cases.

In practice, industrial models are reduced to smaller ones with reduction methods. In these cases, the evaluation of nonlinear reduced terms can prove difficult. Indeed, the direct application of the projection basis onto the full numerical model to extract the nonlinear terms may be time-consuming. One solution is to estimate *a priori* the nonlinear reduced forces associated with the reduction basis. That is the purpose of the STiffness Evaluation Procedure (STEP) [12].

Moreover, obtaining the harmonic response of dynamical systems is of particular interest and the Harmonic Balance Method (HBM) is a relevant tool for achieving this goal. Avoiding transient phase calculation, it is used to find the periodic solution of an ordinary differential equation that guarantees significant time-cost reductions in comparison with classical direct time integration methods. HBM is often completed by a continuation technique. These approaches enhance the following solution branches and optimize time-cost reduction.

In this paper, we propose a study of the internal resonances of a reduced industrial blade model subjected to large geometrical deflection. The reduction is performed by modal projection. The nonlinear stiffnesses are determined by a STiffness Evaluation Procedure (STEP) and the simulations are performed using HBM coupled with a pseudo arc-length continuation procedure.

1 NUMERICAL APPROACH

In the following, the equations of motion of an n -degrees-of-freedom (DOFs) system subjected to geometrical nonlinearities are written in the form:

$$\mathbf{M}\ddot{\mathbf{x}}(t) + \mathbf{C}\dot{\mathbf{x}}(t) + \mathbf{K}\mathbf{x}(t) + \mathbf{f}^{\text{nl}}(\mathbf{x}(t)) = \mathbf{f}^{\text{ext}}(t) \quad (2)$$

where $\mathbf{x}(t)$ is the vector of unknown displacements, \mathbf{M} , \mathbf{C} , \mathbf{K} are the usual structural matrices, i.e. mass, damping and stiffness, respectively. The $\mathbf{f}^{\text{nl}}(\mathbf{x}(t))$ vector refers to the geometrical nonlinear terms. Finally $\mathbf{f}^{\text{ext}}(t)$ is the vector of external forces acting on the system.

1.1 Reduction

For industrial models, the size of the system (2) is generally large and calculation costs quickly reach prohibitive levels. To overcome this difficulty, reduction methods are generally employed to restrict the number of unknowns

and lead to appropriately sized systems. In this paper, the reduction is carried out by classical modal projection using the linear normal modes (LNM) Φ_i of the underlying undamped linear system of Eqn. (2). To this end, matrix Φ including a subset of r eigenvectors is introduced to expand the displacement vector as follows:

$$\mathbf{x}(t) = \Phi \mathbf{q}(t) \quad (3)$$

Substituting this expression in Eqn. (2) leads to,

$$\widetilde{\mathbf{M}}\ddot{\mathbf{q}}(t) + \widetilde{\mathbf{C}}\dot{\mathbf{q}}(t) + \widetilde{\mathbf{K}}\mathbf{q}(t) + \Phi^T \mathbf{f}^{\text{nl}}(\Phi \mathbf{q}(t)) = \widetilde{\mathbf{f}}^{\text{ext}}(t) \quad (4)$$

where

$$\begin{aligned} \widetilde{\mathbf{M}} &= \Phi^T \mathbf{M} \Phi \\ \widetilde{\mathbf{C}} &= \Phi^T \mathbf{C} \Phi \\ \widetilde{\mathbf{K}} &= \Phi^T \mathbf{K} \Phi \\ \widetilde{\mathbf{f}}^{\text{ext}}(t) &= \Phi^T \mathbf{f}^{\text{ext}}(t) \end{aligned} \quad (5)$$

The size of the reduced system (4) is r with $r \ll n$. Generally, the expressions of the nonlinear terms in Eqn. (2) are not available since they originate from a finite element program. Their expression in Eqn. (4) is therefore unknown. The stiffness evaluation procedure (STEP) allows overcoming this difficulty.

1.2 STiffness Evaluation Procedure (STEP)

The STiffness Evaluation Procedure is a method for determining the nonlinear modal stiffness coefficients from an arbitrary finite element model. The principle is to assume the expression of the nonlinear reduced modal forces in the following form [12],

$$\Phi^T \mathbf{f}^{\text{nl}}(\Phi \mathbf{q}(t)) = \sum_{j=1}^r \sum_{k=j}^r \mathbf{K}_{jk}^q q_j q_k + \sum_{j=1}^r \sum_{k=j}^r \sum_{l=k}^r \mathbf{K}_{jkl}^c q_j q_k q_l \quad (6)$$

where \mathbf{K}^q and \mathbf{K}^c are second and third order tensors whose components are quadratic and cubic nonlinear stiffness coefficients. Then, the method proposed in [12] suggests determining the unknown coefficients \mathbf{K}_{jk}^q and \mathbf{K}_{jkl}^c using a series of prescribed nodal displacements \mathbf{x}_p . The procedure is summarized as follows.

By assuming the nodal displacement along one of the linear eigenvectors Φ_j , $\mathbf{x}_p = \Phi_j q_j$, coefficients \mathbf{K}_{jj}^q and \mathbf{K}_{jjj}^c associated with the nonlinear modal restoring force can be isolated in Eqn. (7),

$$\Phi^T \mathbf{f}^{\text{nl}}(\Phi_j q_j) = \mathbf{K}_{jj}^q q_j q_j + \mathbf{K}_{jjj}^c q_j q_j q_j \quad (7)$$

Then, by employing another displacement expression, $\mathbf{x}_p = \Phi_j q_j + \Phi_k q_k$, a new relationship can be obtained between the coefficients $\mathbf{K}_{jk}^q q_j q_k$, $\mathbf{K}_{jjk}^c q_j q_j q_k$ and $\mathbf{K}_{jkk}^c q_j q_k q_k$ and the nonlinear modal force,

$$\begin{aligned} \Phi^T \mathbf{f}^{\text{nl}}(\Phi_j q_j + \Phi_k q_k) &= \mathbf{K}_{jj}^q q_j q_j + \mathbf{K}_{jjj}^c q_j q_j q_j + \mathbf{K}_{kk}^q q_k q_k \\ &+ \mathbf{K}_{kkk}^c q_k q_k q_k + \mathbf{K}_{jk}^q q_j q_k + \mathbf{K}_{jjk}^c q_j q_j q_k + \mathbf{K}_{jkk}^c q_j q_k q_k \end{aligned} \quad (8)$$

Finally, coefficients \mathbf{K}_{jkl}^c are obtained by enforcing the displacement \mathbf{x}_p to be equal to $\Phi_j q_j + \Phi_k q_k + \Phi_l q_l$, leading to the following equation,

$$\begin{aligned} \Phi^T \mathbf{f}^{\text{nl}}(\Phi_j q_j + \Phi_k q_k + \Phi_l q_l) &= \mathbf{K}_{jj}^q q_j q_j + \mathbf{K}_{kk}^q q_k q_k + \mathbf{K}_{ll}^q q_l q_l \\ &+ \mathbf{K}_{jk}^q q_j q_k + \mathbf{K}_{jl}^q q_j q_l + \mathbf{K}_{kl}^q q_k q_l + \mathbf{K}_{jjj}^c q_j q_j q_j + \mathbf{K}_{kkk}^c q_k q_k q_k \\ &+ \mathbf{K}_{lll}^c q_l q_l q_l + \mathbf{K}_{jjk}^c q_j q_j q_k + \mathbf{K}_{kjj}^c q_k q_j q_j + \mathbf{K}_{jjl}^c q_j q_j q_l \\ &+ \mathbf{K}_{llj}^c q_l q_l q_j + \mathbf{K}_{kkj}^c q_k q_k q_j + \mathbf{K}_{llk}^c q_l q_l q_k + \mathbf{K}_{jkl}^c q_j q_k q_l \end{aligned} \quad (9)$$

Coefficients \mathbf{K}_{jk}^q and \mathbf{K}_{jkl}^c are determined by combining Eqns.(7), (8) and (9). For instance, the unknowns \mathbf{K}_{jj}^q can be obtained by summing $\Phi^T \mathbf{f}^{nl}(\Phi_j q_j)$ and $\Phi^T \mathbf{f}^{nl}(-\Phi_j q_j)$. In the same manner, subtracting $\Phi^T \mathbf{f}^{nl}(\Phi_j q_j)$ and $\Phi^T \mathbf{f}^{nl}(-\Phi_j q_j)$ enables computing coefficients \mathbf{K}_{jjj}^c .

1.3 Harmonic Balance Method

A harmonic balance strategy was developed [13] to estimate the nonlinear response of the nonlinear dynamical equations. The principle of the Harmonic Balance Method (HBM) is to approximate the periodic solution of an ordinary differential equation using a truncated Fourier series:

$$\mathbf{x}(t) = \mathbf{a}_0 + \sum_{k=1}^{N_h} \mathbf{a}_k \cos(k\omega t) + \mathbf{b}_k \sin(k\omega t) \quad (10)$$

Substituting Eqn. (10) and its derivatives in the equations of motion and projecting the resulting expression, using the Galerkin method [14], onto the harmonic function basis $\mathcal{B} = \{1, \cos(k\omega t), \sin(k\omega t), k = 1 \dots N_h\}$ by way of the following scalar product,

$$\langle f(t), g(t) \rangle = \frac{\omega}{\pi} \int_0^{\frac{2\pi}{\omega}} f(t)g(t)dt \quad (11)$$

yields the nonlinear algebraic system,

$$\mathbf{Z}(\omega)\hat{\mathbf{x}} + \hat{\mathbf{f}}^{nl}(\hat{\mathbf{x}}) = \hat{\mathbf{f}}^{ext} \quad (12)$$

where $\hat{\mathbf{x}}$ is the vector of unknowns $[\mathbf{a}_0^T, \mathbf{a}_1^T, \mathbf{b}_1^T, \dots]^T$, $\hat{\mathbf{f}}^{nl}$ and $\hat{\mathbf{f}}^{ext}$ are the Fourier coefficients of \mathbf{f}^{nl} and \mathbf{f}^{ext} . \mathbf{Z} is the so-called *dynamic stiffness matrix* defined by,

$$\mathbf{Z} = \begin{bmatrix} 2\mathbf{K} & & & \\ & \mathbf{Z}_1 & & \\ & & \ddots & \\ & & & \mathbf{Z}_{N_h} \end{bmatrix}, \quad \mathbf{Z}_k = \begin{bmatrix} \mathbf{K} - (k\omega)^2 \mathbf{M} & k\omega \mathbf{C} \\ -k\omega \mathbf{C} & \mathbf{K} - (k\omega)^2 \mathbf{M} \end{bmatrix} \quad (13)$$

In spite of its limitation to harmonic solutions, the harmonic balance method is a useful method since no hypotheses are made concerning the transient phase of the response. Indeed, the latter is ignored during the procedure. Furthermore, despite the increase of unknowns, the resolution of an algebraic system offers a significant reduction in computational costs compared to traditional time integration methods.

1.4 Alternating Frequency Time (AFT)

Determining the Fourier coefficients $\hat{\mathbf{f}}^{nl}(\hat{\mathbf{x}})$ in Eqn. (10) is generally not straightforward except in some rare cases where analytical expressions can be derived. Even in these cases, the Alternating Frequency/Time (AFT) procedure is generally preferred. The AFT method allows computing the coefficients required by transposing frequency-domain terms in the time-domain terms [15]. The general procedure, recalled by Eqn. (14), is summarized as follows. By expressing $\hat{\mathbf{x}}$ in time space using inverse discrete Fourier transform (iDFT), allows evaluating the nonlinear forces, after which the Fourier coefficients of the nonlinear forces in frequency space are derived using the direct Fourier transform (DFT).

$$\hat{\mathbf{x}} \xrightarrow{\text{iDFT}} \mathbf{x}(t) \longrightarrow \mathbf{f}^{nl}(\mathbf{x}(t)) \xrightarrow{\text{DFT}} \hat{\mathbf{f}}^{nl}(\hat{\mathbf{x}}) \quad (14)$$

As an algebraic nonlinear system, Eqn. (12) can be solved using usual Newton-like methods for which an analytical expression of the Jacobian is required. Using both the AFT procedure and the composed function derivation rule, the computation of the first derivatives of the nonlinear terms can be done easily by applying Eqn. (15),

$$\frac{\partial \hat{\mathbf{f}}^{nl}}{\partial \hat{\mathbf{x}}} = \mathbf{F} \frac{\partial \mathbf{f}^{nl}}{\partial \mathbf{x}} \bar{\mathbf{F}} \quad (15)$$

where \mathbf{F} (resp. $\bar{\mathbf{F}}$) stands for the DFT (resp. iDFT). Note that nonlinear terms are independent of ω since the nonlinearity is purely displacement dependent.

Most of the time, system (12) is extended so as to include a parametrization equation to ensure the continuation of the solution branch.

1.5 Continuation

Continuation or path following methods consist in finding a set of solutions of a system by varying a parameter called *continuation parameter* [16]. In frequency response analysis, this parameter often corresponds to the system excitation frequency Ω . The most common continuation methods rely on a *predictor-corrector* scheme.

Geometrical nonlinear systems often exhibit multiple solution branches featuring bifurcation points such as turning points (TP) and branching points (BP) (Fig. 1). For such dynamical systems, predictor/corrector approaches such as sequential continuation generally fail to track solution branches. To overcome turning point failures, branches of solutions are parametrized by the arc-length parameter s , that is, $(\mathbf{x}, \Omega) = (\mathbf{x}(s), \Omega(s))$. A wide range of predictor/corrector methods using arc-length parametrization are available in the literature [17]. In this paper, the estimated solutions are computed with tangent prediction while the correction uses the pseudo arc-length method [18].

The pseudo arc-length method forces the corrected point to belong to a hyperplane orthogonal to the tangent prediction vector (Fig. 1). Assuming that the equations of the predicted point are:

$$\begin{aligned} \mathbf{x}_{i+1}^{\text{pre}} &= \mathbf{x}_i + \Delta \mathbf{x} \\ \omega_{i+1}^{\text{pre}} &= \omega_i + \Delta \omega \end{aligned} \quad (16)$$

with $\mathbf{t} = [\Delta \mathbf{x}^\top, \Delta \omega]^\top$ the tangent to the branch at previous solution point $[\mathbf{x}_i^\top, \omega_i]^\top$ and $[\mathbf{x}_{i+1}^{\text{pre}^\top}, \omega_{i+1}^{\text{pre}}]^\top$ the prediction of the next solution point, pseudo arc-length is reduced to:

$$\begin{bmatrix} \mathbf{x}_{i+1} - \mathbf{x}_{i+1}^{\text{pre}} \\ \omega_{i+1} - \omega_{i+1}^{\text{pre}} \end{bmatrix}^\top \cdot \mathbf{t} = 0 \quad (17)$$

or equivalently,

$$\begin{aligned} (\mathbf{x}_{i+1} - \mathbf{x}_i)^\top \Delta \mathbf{x} + (\omega_{i+1} - \omega_i) \Delta \omega - \Delta s^2 &= 0 \\ \Delta \omega^2 + \Delta \mathbf{x}^\top \Delta \mathbf{x} &= \Delta s^2 \end{aligned} \quad (18)$$

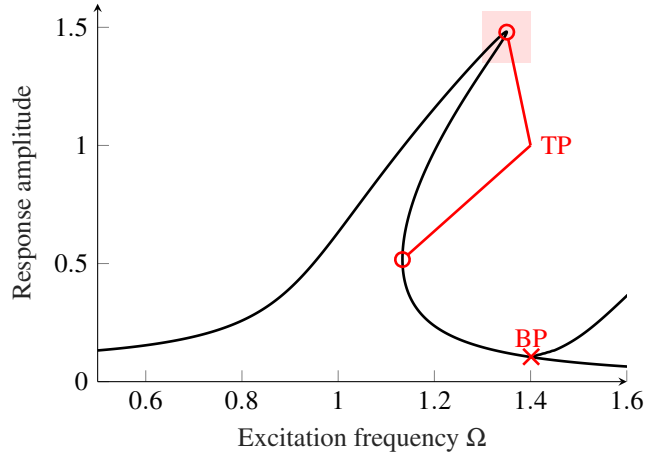
with $\Delta s = \|\mathbf{t}\|$.

Pseudo arc-length continuation is carried on by appending Eqn. (18) to Eqn. (12), leading to the so-called *extended system*.

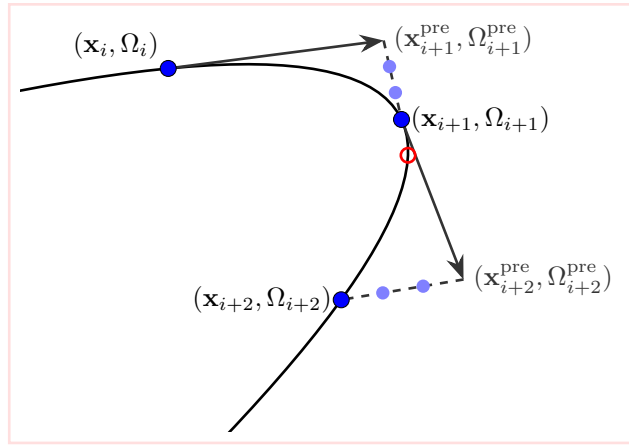
1.6 Bifurcation

As mentioned earlier, nonlinear systems can exhibit nonlinear phenomena such as bifurcation points. They appear at points for which the Jacobian of the system becomes singular [19]. Although turning points (TP) are automatically computed thanks to arc-length parametrization, branching points (BPs) are tricky to handle [20]. At the same time, since internal resonances originate from BP [2], being able to predict them and follow bifurcated branches is of particular interest for our study. In the following we denote the nonlinear system as $\mathbf{f}(\mathbf{x}, \omega)$ and assume that its size is equal to n . BP analysis can be summarized in 3 steps:

1. Localization of the BP
2. Resolution of the branching system;
3. Computation of the bifurcated branches.



(a) Branches of solutions



(b) Close-up near turning point region

Fig. 1: NONLINEAR FREQUENCY RESPONSE. (A) BIFURCATION POINTS: TURNING POINTS [○], BRANCHING POINTS [×]. (B) PSEUDO ARC-LENGTH CONTINUATION: SOLUTION POINTS [●], ITERATION POINTS [◐]

The first step relies on monitoring the determinant of the Jacobian $\mathbf{f}_x (= \partial \mathbf{f} / \partial \mathbf{x})$ of the system. A change of sign of this determinant for two consecutive solution points indicates the presence of a bifurcation point. This step is similar for both the turning and the branching points. The type of bifurcation is determined along with the next step. The second step is aimed at finding the exact position of the previously identified bifurcation point. This procedure is performed using the so-called *branching system* [21],

$$\begin{bmatrix} \mathbf{f}(\mathbf{x}, \omega) \\ \mathbf{f}_x(\mathbf{x}, \omega) \mathbf{h} \\ \|\mathbf{h}\| - 1 \end{bmatrix} = \mathbf{0} \quad (19)$$

where \mathbf{h} is a nontrivial eigenvector associated with the null eigenvalue of $\mathbf{f}_x(\mathbf{x}, \omega)$. The type of bifurcation is determined by the rank of the rectangular matrix $[\mathbf{f}_x \ \mathbf{f}_\omega]$ ($= [\partial \mathbf{f} / \partial \mathbf{x}, \partial \mathbf{f} / \partial \omega]$). For a full rank n the bifurcation is a turning point, while for a rank at most equal to $n - 1$ the bifurcation is a branching point and it is necessary to go on with step 3. An alternative to the system (19), is described in [22]. It prevents the singularity of the Jacobian of the system (19) near BPs. This approach was used in this document. The last step consists in determining the branches emanating from the identified BP. This can be done by applying a branch switching algorithm whose procedure is fully described by Kuznetsov in [23]. Here, we briefly present the main idea of the branch switching algorithm.

The purpose of the method is to determine the tangents to the branches at the branching point. For the sake of simplicity, we here consider the case of only two emanating branches. In the following, we define $\mathbf{y} := (\mathbf{x}, \omega)$ and

denote by superscript '0' variables at the branching points. A BP will hence be noted \mathbf{y}^0 . Kuznetsov showed that the tangents can be written in the form,

$$\mathbf{t} = \beta_1 \mathbf{q}_1 + \beta_2 \mathbf{q}_2 \quad (20)$$

with $(\beta_1, \beta_2) \in \mathbb{R}^2$ and $\{\mathbf{q}_1, \mathbf{q}_2\} = \text{span}\{\text{Ker}(\mathbf{f}_{\mathbf{y}}(\mathbf{y}^0))\}$. Supposing the null-space of $\mathbf{f}_{\mathbf{y}}$ at the BP already identified, the definition of the tangents resumes to determine the values of the coefficients β_1 and β_2 in Eqn. (20). As demonstrated in [23], they are the solution of the quadratic form system,

$$\begin{aligned} b_{11}\beta_1^2 + 2b_{12}\beta_1\beta_2 + b_{22}\beta_2^2 &= 0 \\ \text{with } b_{ij} &= \langle \varphi, \mathbf{B}(\mathbf{q}_i, \mathbf{q}_j) \rangle, \quad i, j = 1, 2 \end{aligned} \quad (21)$$

with φ belonging to the null-space of $\mathbf{f}_{\mathbf{y}}^T(\mathbf{y}^0)$ and \mathbf{B} being the second order derivative of \mathbf{f} (i.e. the Hessian). The scalar product in Eqn. (21) is defined as follows,

$$\langle \varphi, \mathbf{B}(\mathbf{q}, \mathbf{q}) \rangle = \sum_{i=1}^n \sum_{j,k=1}^{n+1} \varphi_i \left. \frac{\partial^2 \mathbf{f}_i(\mathbf{y})}{\partial y_j \partial y_k} \right|_{\mathbf{y}=\mathbf{y}^0} q_j q_k \quad (22)$$

The second order system (21) possesses 2 independent nontrivial solutions if $b_{11}b_{22} - b_{12}^2 < 0$. These two solutions correspond to the two desired tangents. By diagonalizing the matrix associated with the quadratic form of Eqn. (21), it is possible to express β_1 in terms of β_2 . The values of these two coefficients will be estimated by enforcing the norm of the tangent vectors.

2 APPLICATION FOR AN INDUSTRIAL MODEL

2.1 Presentation of the industrial blade model

The model considered for the application of the numerical methods described previously is a finite element industrial blade model. The blade, composed of 59765 DOFs, is shown in Fig. 2.

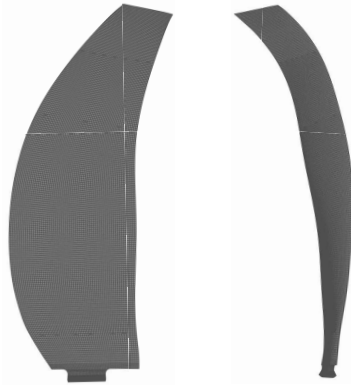


Fig. 2: FINITE ELEMENT MODEL OF THE INDUSTRIAL BLADE

As recalled in the introduction of this document, slender components such as engine blades can undergo large displacements leading to nonlinear behavior. Here, we focus on a particular feature of nonlinear systems, namely internal resonance. In particular we focus on the first torsional mode and the second bending mode whose linear eigenfrequencies are nearly commensurable, so that $\omega_2 \simeq 2\omega_1$.

2.2 Model reduction and hypothesis

As we are dealing with an industrial blade model, the number of DOFs is too large to carry out the nonlinear analysis planned in this paper. Consequently, the blade model must be reduced. This reduction was performed

Table 1: MODAL QUADRATIC AND CUBIC STIFFNESS COEFFICIENTS OF THE REDUCED MODEL

Modal Equation	1	2
K_{11}^q	8.79×10^3	-9.04×10^3
K_{12}^q	-1.81×10^4	3.83×10^4
K_{22}^q	1.91×10^4	-1.97×10^4
K_{111}^c	5.85×10^6	-3.24×10^6
K_{112}^c	-9.73×10^6	1.66×10^7
K_{122}^c	1.66×10^7	-1.42×10^7
K_{222}^c	-4.72×10^6	1.51×10^7

using the procedure presented in the first part of the present document. Since we are interested in the interaction between the first torsional mode and the second bending mode of the blade, the reduction basis is composed only of these two modes. The resulting reduced model therefore depends on two generalized coordinates denoted q_1 and q_2 .

To complete the reduced model, the following hypotheses are made. First, we assume an external force in the form of a punctual cosine excitation with pulsation Ω and amplitude F_0 acting on the blade tip. The damping matrix is assumed to be diagonal with a damping ratio ζ_1 equal to 0.02% for the first mode and ζ_2 equal to 0.016% for the second mode. Finally, the reduced stiffnesses are computed using the STEP method with prescribed displacements $q_j = 1 \times 10^{-2}$ and $q_k = 5 \times 10^{-2}$ in Eqns. (7) and (8). The nonlinear stiffness coefficients obtained using the STEP method are given in Tab. 1. It is important to point out that a set of values ranging from 1×10^{-2} to 1×10^1 was used for the prescribed modal displacements q_j and q_k . For each choice, the STEP simulations provided very similar results. Besides, these choices of modal displacements correspond to a deflection magnitude at blade tip ranging from 0.1 mm to around 5 cm. These remarks highlight the great stability of the STEP method and its potential for handling large nonlinearities. Tab. 1, clearly shows that reduced cubic stiffness coefficients are predominant in comparison with the quadratic coefficients. The reduced model has the form of Eqn. (4), and in the rest of this article we consider the two pulsations ω_1 and ω_2 such that $\omega_2 \simeq 2\omega_1$.

In the following, the frequency response of the model is analyzed near the two pulsations of the reduced system using the numerical methods presented in the first part. Results in physical coordinates are retrieved using the modal projection (3) and vibration motion is studied at blade tip. Particular attention is given to the computation of bifurcated branches. All the pulsations will be made dimensionless with respect to the first pulsation of the system and the dimensionless variables will be denoted by superscript '*'.

2.3 Numerical results

2.3.1 Excitation near ω_1

The frequency response at blade tip corresponding to an excitation of amplitude $F_0 = 0.015$ N around the first pulsation ω_1 of the reduced model is shown in Fig. 3. The simulation was carried out with $N_h = 5$ harmonics in the Fourier series decomposition and 128 time-steps for the AFT procedure. Due to the predominance of reduced cubic stiffness coefficients, the frequency response exhibits a significant stiffening effect.

The evolution of the Fourier coefficients of the response at blade tip for points (a) to (d) (Fig. 3) is depicted in Fig. 4. Starting from point (a), the response is linear with an harmonic 1 dominant compared to the others. For point (b) near $\Omega^* = 1$ the second harmonic begins to participate in the response. The first effects of the 2 to 1 internal resonance occur. From (b) to (c) the relative level of the second harmonic grows with the excitation pulsation. Finally from (c) to (d) the presence of the harmonic 2 stops i.e. the effects of the internal resonance cease and only the fundamental harmonic responds to the excitation.

The internal resonance occurrence can be further characterized by observing the temporal signal of the two generalized coordinates $q_1(t)$ and $q_2(t)$ for points (a) to (d) (Fig. 5). The signals were obtained by applying the inverse discrete Fourier transform on the Fourier coefficients. From (a) to (b) the signals are in phase with a

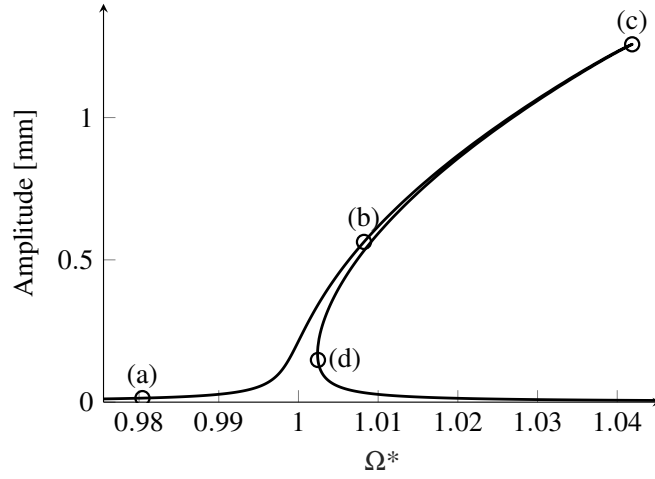


Fig. 3: FREQUENCY RESPONSE AT BLADE TIP NEAR ω_1

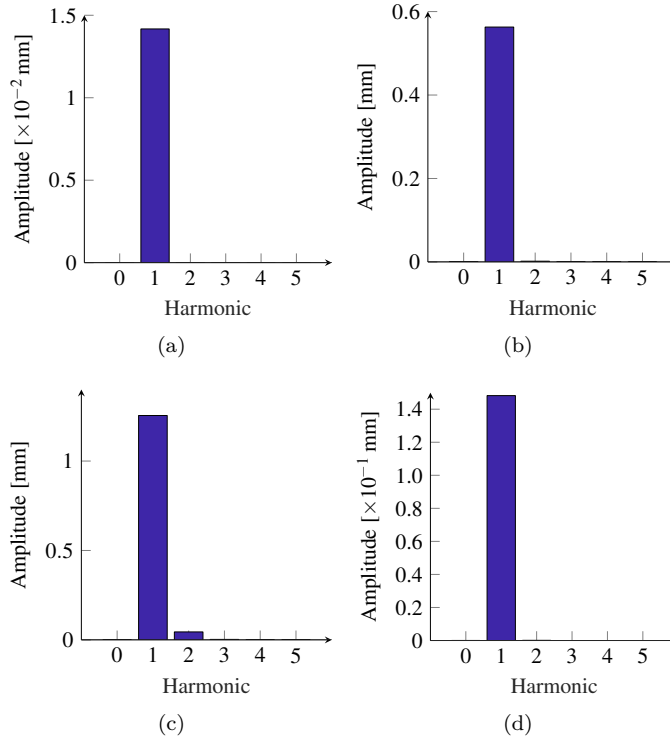


Fig. 4: FOURIER COEFFICIENTS $\left(\sqrt{\mathbf{a}_k^2 + \mathbf{b}_k^2}\right)$ OF THE RESPONSE AT BLADE TIP FOR AN EXCITATION CLOSE TO ω_1

pulsation corresponding to the fundamental harmonic of the excitation. For both signals, harmonic 1 is dominant. From (b) to (c) the nonlinear coupling between the modal coordinates allows q_2 to vibrate with a pulsation equal to the double of the excitation pulsation. Harmonic 2 in q_2 becomes dominant over harmonic 1. This situation clearly shows that the internal resonance acts on the second mode of the reduced system. From (c) to (d) the signals get back to an harmonic 1 response.

Hence, the characteristics of the nonlinear system permits the occurrence of a 2 to 1 internal resonance. In other words, when the excitation is close to ω_1 the intrinsic nonlinear behavior of the reduced system activates the internal resonance and harmonic 2 of the excitation appears in the response.

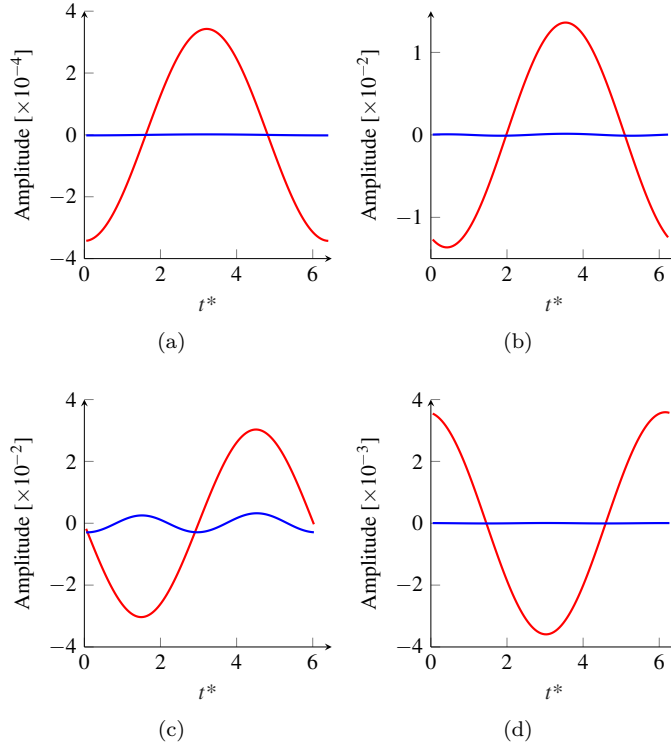


Fig. 5: TEMPORAL SIGNALS OF THE MODAL COORDINATES $q_1(t)$ [—] AND $q_2(t)$ [—]

2.3.2 Excitation near ω_2

Let us now focus on the frequency response at blade tip for an excitation around the second pulsation of the reduced system. The response was obtained with a force amplitude $F_0 = 0.10$ N and the results are shown in Fig. 6. It is important to note that we here expect a response with a pulsation equal to half the pulsation of the excitation. Hence, we consider a pulsation of excitation in the form 2Ω with Ω close to $\omega_2/2$. In this manner, in absence of internal resonance, only harmonic 2 responds to the excitation. As in the previous case, the curve still exhibits

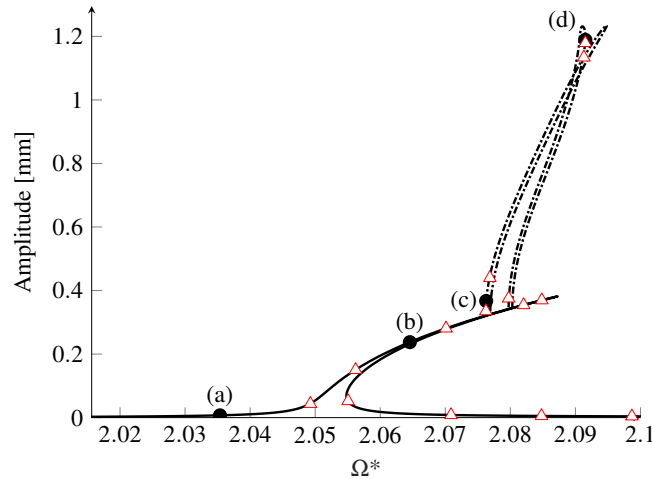


Fig. 6: FREQUENCY RESPONSE AT BLADE TIP NEAR ω_2 . PRINCIPAL BRANCH [—], SECONDARY BRANCH [---]. TEMPORAL INTEGRATION [Δ]

a stiffening behavior. However, contrary to the previous case, two bifurcated branches of solutions can be seen near the high amplitudes. These branches, referred to as secondary branches, were computed using the algorithm

presented in section 1.6. Branches with commensurable shapes were observed in [24]. It is noteworthy that the branches reach high amplitudes for a very small range of pulsations. A first conclusion can be drawn; in conception phase, missing the secondary branches can lead to underestimate the level of vibration.

Because of the atypical shapes of the response branches, we wished to validate our results by a temporal method. Thus, a temporal integration method using an explicit Runge-Kutta formula was performed on the reduced model and initial conditions was chosen close to the harmonic balance results. Results for several excitation pulsations are superimposed to the frequency response in Fig. 6. Results present a very good correlation for the principal branch of solution as well as the secondary branches. Then, the comparison enables to validate the results obtained by HBM. Note that owing to probable instability purposes, only a few solution points were obtained on the secondary branches.

The evolution of the Fourier coefficients at blade tip for four chosen solution points was determined. It is illustrated in Fig. 7(a) to (d). On the principal branch of solutions, only harmonic 2 participates in the response

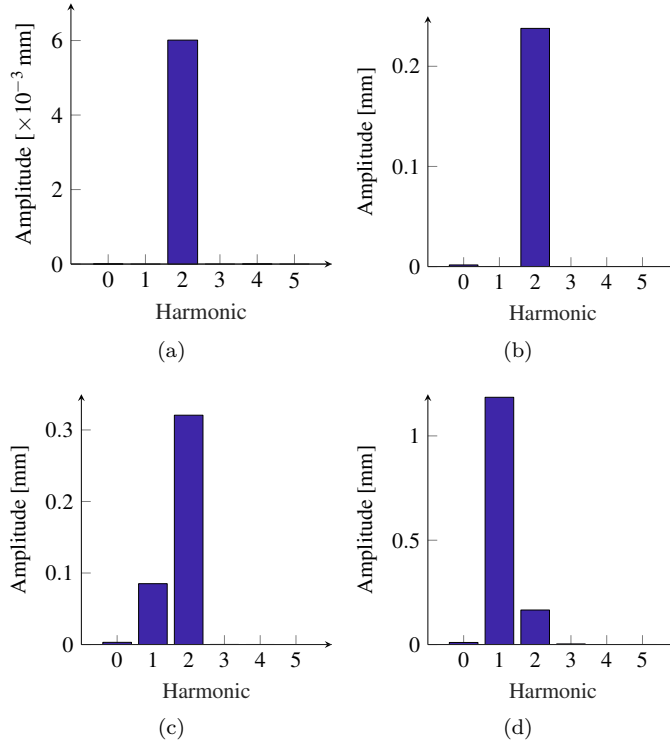


Fig. 7: FOURIER COEFFICIENTS $\left(\sqrt{\mathbf{a}_k^2 + \mathbf{b}_k^2}\right)$ OF THE RESPONSE AT BLADE TIP FOR AN EXCITATION CLOSE TO ω_2

(harmonic 0 also participates but at a much smaller level). For this branch, no internal resonance occurs (Fig. 7 (a) and (b)). However, on the first and second bifurcated branches (points (c) and (d)), the first harmonic participates in the frequency response (Fig. 7(c) and (d)). Thus, a 2 to 1 internal resonance occurs for secondary branches. In addition, the amplitude of harmonic 1 grows along the secondary branches and can be considerably superior than the amplitude of the second harmonic (Fig. 7(d)). Thus, in contrast with the first case of excitation, the internal resonance only occurs for bifurcated branches.

Again, an overview of the temporal signals of the modal coordinates q_1 and q_2 helps understanding of the transition from classical nonlinear interaction to the occurrence of internal resonance (Fig. 8). For points belonging to the principal branch of solutions, both $q_1(t)$ and $q_2(t)$ respond with the harmonic of the excitation, corresponding to harmonic 2 (Fig. 8(a) and (b)). By examining the signals in Fig. 8(c) and (d), it is clear that $q_1(t)$ responds with the first harmonic while $q_2(t)$ responds with the second harmonic. Thus, internal resonance impacts the dynamic of the first modal coordinate. In addition, Fig. 8(d) shows that for an excitation case close to ω_2 , the response amplitude of $q_1(t)$ can be higher than the amplitude of $q_2(t)$.

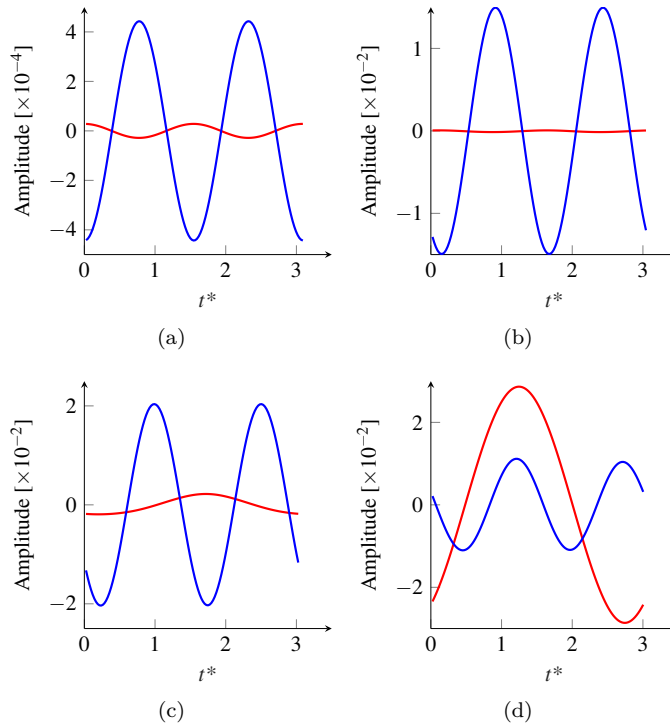


Fig. 8: TEMPORAL SIGNALS OF THE MODAL COORDINATES $q_1(t)$ [—] AND $q_2(t)$ [—]

3 CONCLUSION

Large engine components such as fan blades may undergo large geometrical deflection due to their slender shape. This behavior implies serious nonlinear effects whose comprehension is essential for designers. Indeed, these effects may significantly alter the linear behavior of the structures. One feature of nonlinear effects is the internal resonance phenomenon which, involving modes coupling, can increase vibratory levels. Thus, their prediction and identification in conception phase represents an important challenge for industrial designers.

In this paper, the nonlinear harmonic response of an industrial blade model undergoing large deflection has been studied. For computational purposes, the model has been reduced using the linear normal modes of the structure. Nonlinear effects have been taken into account through polynomial stiffnesses and reduced nonlinear stiffness coefficients were obtained by a stiffness evaluation procedure. The harmonic balance method coupled to a pseudo arc-length continuation approach has been used to determine the periodic solutions of the nonlinear dynamic system. During the simulations, attention has been paid to internal resonance risks.

Excitations close to the first and second mode of the reduced model have been studied. In both cases, frequency response at blade tip has been obtained by modal projection. In the first case, the internal resonance was activated as soon as the excitation pulsation reached the pulsation of the first mode. In this case the response of the second mode initiated with a pulsation equal to two times the excitation pulsation. In the second case, internal resonance occurred through secondary branches of solutions computed by a branch switching method. On these branches, participation of harmonic 1 corresponding to half the harmonic of the excitation has been observed. The atypical behavior of the frequency response has been verified thanks to temporal integration. The comparison has permitted to validate the results obtained by the harmonic balance method.

The study presented in this document has been conducted on a significantly reduced model, however this paper highlights the potential of the described methods to predict internal resonance phenomena for an industrial model with the harmonic balance method. In further works, it would be interesting to complete the reduction basis using, for instance, modal derivatives [25].

Acknowledgements

The authors would like to thank Safran Aircraft Engines for providing the financial support for this project, and for giving permission to publish this work.

References

- [1] Nayfeh, A. H., and Mook, D. T., 1979. “Nonlinear oscillations”. *Nonlinear oscillations, by Nayfeh, Ali Hasan; Mook, Dean T.* New York: Wiley, c1979.
- [2] Kerschen, G., Peeters, M., Golinval, J.-C., and Vakakis, A. F., 2009. “Nonlinear normal modes, part i: A useful framework for the structural dynamicist”. *Mechanical Systems and Signal Processing*, **23**(1), pp. 170–194.
- [3] Nayfeh, A. H., Mook, D. T., and Marshall, L. R., 1973. “Nonlinear coupling of pitch and roll modes in ship motions”. *Journal of Hydronautics*, **7**(4), pp. 145–152.
- [4] Haddow, A., Barr, A., and Mook, D., 1984. “Theoretical and experimental study of modal interaction in a two-degree-of-freedom structure”. *Journal of Sound and Vibration*, **97**(3), pp. 451–473.
- [5] Boivin, N., Pierre, C., and Shaw, S., 1995. “Non-linear modal analysis of structural systems featuring internal resonances”. *Journal of Sound and Vibration*, **182**(2), pp. 336–341.
- [6] Jiang, D., Pierre, C., and Shaw, S., 2005. “The construction of non-linear normal modes for systems with internal resonance”. *International Journal of Non-Linear Mechanics*, **40**(5), pp. 729–746.
- [7] Pesheck, E., Boivin, N., Pierre, C., and Shaw, S. W., 2001. “Nonlinear modal analysis of structural systems using multi-mode invariant manifolds”. *Nonlinear Dynamics*, **25**(1-3), pp. 183–205.
- [8] Peeters, M., Vigié, R., Sérandour, G., Kerschen, G., and Golinval, J.-C., 2009. “Nonlinear normal modes, part ii: Toward a practical computation using numerical continuation techniques”. *Mechanical systems and signal processing*, **23**(1), pp. 195–216.
- [9] King, M., and Vakakis, A., 1996. “An energy-based approach to computing resonant nonlinear normal modes”. *Journal of Applied Mechanics*, **63**(3), pp. 810–819.
- [10] Ribeiro, P., and Petyt, M., 1999. “Non-linear vibration of beams with internal resonance by the hierarchical finite-element method”. *Journal of Sound and vibration*, **224**(4), pp. 591–624.
- [11] Ribeiro, P., and Petyt, M., 2000. “Non-linear free vibration of isotropic plates with internal resonance”. *International Journal of Non-Linear Mechanics*, **35**(2), pp. 263–278.
- [12] Muravyov, A. A., and Rizzi, S. A., 2003. “Determination of nonlinear stiffness with application to random vibration of geometrically nonlinear structures”. *Computers & Structures*, **81**(15), pp. 1513–1523.
- [13] Krylov, N., and Bogoliubov, N., 1947. “Introduction to non-linear mechanics (am-11)”.
[14] Urabe, M., 1965. “Galerkin’s procedure for nonlinear periodic systems”. *Archive for Rational Mechanics and Analysis*, **20**(2), pp. 120–152.
- [15] Cameron, T., and Griffin, J., 1989. “An alternating frequency/time domain method for calculating the steady-state response of nonlinear dynamic systems”. *Journal of applied mechanics*, **56**(1), pp. 149–154.
- [16] Allgower, E. L., and Georg, K., 2012. *Numerical continuation methods: an introduction*, Vol. 13. Springer Science & Business Media.
- [17] Nayfeh, A. H., and Balachandran, B., 1995. “Applied nonlinear dynamics: analytical, computational and experimental methods”. *Wiley series in nonlinear science, New York; Chichester: Wiley, — c1995*.
- [18] Keller, H. B., 1977. “Numerical solution of bifurcation and nonlinear eigenvalue problems”. *Application of bifurcation theory*, pp. 359–384.
- [19] Seydel, R., 2009. *Practical bifurcation and stability analysis*, Vol. 5. Springer Science & Business Media.
- [20] Grolet, A., and Thouverez, F., 2010. “Vibration analysis of a nonlinear system with cyclic symmetry”. In ASME Turbo Expo 2010: Power for Land, Sea, and Air, American Society of Mechanical Engineers, pp. 917–929.
- [21] Moore, G., and Spence, A., 1980. “The calculation of turning points of nonlinear equations”. *SIAM Journal on Numerical Analysis*, **17**(4), pp. 567–576.
- [22] Xie, L., Bagnuet, S., Prabel, B., and Dufour, R., 2017. “Bifurcation tracking by harmonic balance method for performance tuning of nonlinear dynamical systems”. *Mechanical Systems and Signal Processing*, **88**, pp. 445–461.
- [23] Kuznetsov, Y. A., 2013. *Elements of applied bifurcation theory*, Vol. 112. Springer Science & Business Media.
- [24] Grolet, A., and Thouverez, F., 2012. “On a new harmonic selection technique for harmonic balance method”. *Mechanical Systems and Signal Processing*, **30**, pp. 43–60.
- [25] Martin, A., and Thouverez, F., 2018. “Dynamic analysis and reduction of a cyclic symmetric system subjected to geometric nonlinearities”. In ASME Turbo Expo 2018: Turbomachinery Technical Conference and Exposition, American Society of Mechanical Engineers.